Printed ISSN 1330–0016
Online ISSN 1333–9133
CD ISSN 1333–8390
CODEN FIZBE7

THE CRYSTAL BALL AT MAMI C: RESULTS AND PERSPECTIVES

MICHAEL OSTRICK

Institut für Kernphysik, Universität Mainz, J.J.-Becher Weg 45, 55099 Mainz, Germany

Received 31 January 2011; Accepted 2 November 2011
Online 27 January 2012

The Crystal Ball/TAPS detector setup provides a hermetic photon and hadron calorimeter for the tagged photon facility at the Mainz Microtron accelerator MAMI. High intensity, polarised photon beams of up to 1.5 GeV are used to study photoinduced reactions on nucleons and nuclei. In this article, an overview of the apparatus and selected recent results is given.

PACS numbers: 29.40.Vj, 29.85.Ca UDC 539.1.074

Keywords: photon and hadron calorimeter, Crystal Ball/TAPS detector, study of photoinduced reactions, some recent results

1. Introduction

Electromagnetic probes can be used in a variety of ways and in a wide range of energies, focussing on different aspects of hadron structure and QCD. Below an energy scale of about 3 GeV, the relevant degrees of freedom change from quarks and gluons to mesons and baryons, the bound states of QCD. A characteristic feature in this energy regime is the emergence of scales, e.g. the finite transverse size of hadrons, the dynamic breaking of chiral symmetry and the appearance of discrete resonant states with definite quantum numbers. With the Crystal Ball detector at MAMI, a broad range of experiments are performed in this interesting low-energy regime, where perturbative QCD is not applicable.

2. The Crystal Ball/TAPS detector system at MAMI C

The MAMI accelerator consists of four cascaded microtrons, an injector linac, a thermal source for unpolarised electrons and a laser-driven source for electrons with 80% spin polarisation. The first 3 stages consist of race track microtrons which

deliver beams up to 885 MeV (MAMI B). A fourth stage, the Harmonic Double-Sided Microtron (HDSM) [1], upgrading the maximum energy to 1.6 GeV, came into routine operation in February 2007.

For experiments with circularly and linearly polarised real photons, the Glasgow-Mainz bremsstrahlung tagging facility provides knowledge of the photon energy and flux [2]. Bremsstrahlung is produced by scattering the MAMI electron beam on a thin radiator, while the scattered electrons are separated from the main beam and momentum-analysed by a magnetic dipole spectrometer and a focal-plane detector system made of 353 plastic scintillators. The photons can be energy-tagged in the range from 4.7 to 93.0% of the incident beam energy with a resolution of 2 to 4 MeV and a flux of 2.5×10^5 photons per MeV.

Since 2004, the Crystal Ball calorimeter is the central part of a hermetic detector system. It consists of 672 NaI(Tl) crystals covering 93% of the full solid angle with an energy resolution of 1.7% for electromagnetic showers at 1 GeV. For charged particle tracking and identification, two coaxial multi-wire proportional chambers and a barrel of 24 plastic scintillation counters surrounding the target are installed inside the Crystal Ball sphere. The forward angular range is covered by the TAPS calorimeter consisting of 366 BaF_2 detectors and 72 $PbWO_4$ crystals with higher granularity close to the beam (see Fig. 1).

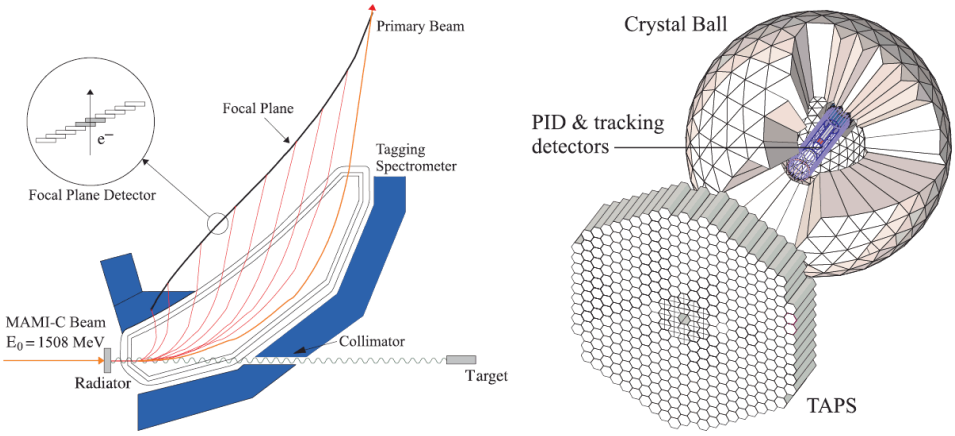

Fig. 1. Left: The Glasgow-Mainz tagging spectrometer. Right: The Crystal Ball/TAPS hermetic calorimeter setup. The cut-away section shows the multi-wire proportional chambers and a barrel of 24 scintillation counters for charged particle identification and tracking.

As spin degrees of freedom are essential, the experimental setup is complemented by polarised targets and a recoil polarimeter. A new Mainz/Dubna frozen-spin target with longitudinal and transverse spin alignment is fully operational at MAMI since the beginning of 2010. It provides up to 90% proton polarisation with relaxation times of about 1500 hours [3].

3. Selected results

3.1. Threshold pion photoproduction

Threshold pion photo-production has long been recognised as a fundamental process arising from the fact that the pion is a Goldstone boson of QCD. Close to the threshold, neutral pion photo-production is dominated by one s-wave, E_{0+}, and three p-wave amplitudes. With this truncation, only a limited number of observables have to be measured for a complete description of the process. Cross section measurements of the $\gamma p \to \pi^0 p$ reaction close to the threshold have been carried out at Mainz [4–6] and Saskatoon [7]. The extracted E_{0+} amplitude shows a strong energy dependence due to the unitary cusp at the opening of the $\gamma p \to \pi^+ n$ reaction threshold. The experimental progress is paralleled by fundamental theoretical efforts. The most recent calculations in heavy baryon ChPT were performed to one loop, or $O(p^4)$ [8]. Other recent calculations start with the $O(p^3)$ chiral Lagrangian and use constraints from unitarity and causality to extend the radius of convergence from the threshold up to the energy region of the $\Delta(1232)$ resonance [9]. Experimentally, a separation of the s-wave amplitude E_{0+} and the three p-wave combinations can be achieved by measuring the photon beam asymmetry

$$\Sigma = \frac{\sigma_\perp - \sigma_{||}}{\sigma_\perp + \sigma_{||}} \tag{1}$$

in addition to the differential cross section. Here $\sigma_\perp$ and $\sigma_{||}$ denote the differential cross sections with the photon polarisation vector perpendicular and parallel to the $p\pi^0$ reaction plane. This asymmetry has recently been measured with the Crystal-Ball/TAPS calorimeter. Figure 2 shows the preliminary results at $\theta_\pi = 90°$

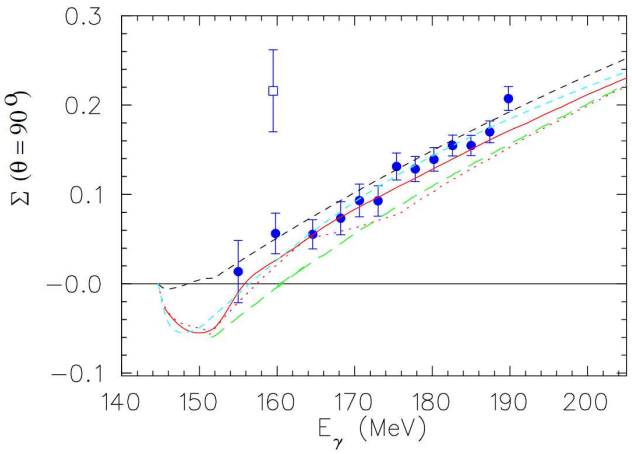

Fig. 2. Preliminary energy dependence of the photon asymmetry Σ at $\theta_{cm} = 90°$ compared to different calculations (solid [11], dashed [9] long dashed [10]) and a pioneering work of Schmidt at al. (open square [6]).

as function of the incoming photon energy. The new results are compared to the pioneering measurement at MAMI by Schmidt et al. in 2001 [6] and different theoretical predictions. The measurement of any further observable will now provide stringent tests of our understanding of the underlying dynamics. In particular, an observation of the time-reversal odd observables, which involve transverse polarised targets, over a larger energy range are needed to understand quantitatively the influence of d-wave amplitudes and to identify the energy scale where ChPT calculations start to become less accurate. A series of data taking periods for π^0 production close to threshold as well as for Compton scattering with transverse proton polarisation is presently being carried out.

3.2. Resonances in photoinduced reactions

A characteristic feature of hadronic reactions below 3 GeV are resonances with well defined quantum numbers. Usually, these resonances are interpreted within models as excitations of three constituent quarks bound in a QCD inspired confining potential. However, there is an increasing number of publications claiming a dynamical origin of resonances due to the strong coupling of meson-baryon channels and thus a molecular nature of these phenomena. A clear interpretation of resonance phenomena is presently obstructed to a large extent by the model dependence of the analysis procedures due to the lack of empirical information about spin observables. All resonances listed in the Particle Data Tables have been identified by model dependent analyses, mainly involving overlapping Breit-Wigner resonances sitting on a non-resonant background. A sensitive check of whether this hypothesis is correct requires the measurement of spin observables dependent on interference terms between different partial wave amplitudes. With the Crystal Ball at MAMI, an experimental program to study all significant spin observables below $W = 2$ GeV has started with the aim to obtain model-independent partial wave analyses of the $\gamma p \to p\pi^0$, $\gamma p \to n\pi^+$ and $\gamma p \to p\eta$ reactions, especially in the energy regions of the $P_{11}(1440)$ and $S_{11}(1535)$ resonances.

The differential cross section for pseudoscalar meson photoproduction with beam and target polarisation is given by

$$\begin{aligned}\frac{\mathrm{d}\sigma}{\mathrm{d}\Omega} &= \sigma_0\Big\{1 - P_T\Sigma\cos 2\varphi + P_x(-P_T H\sin 2\varphi + P_\odot F)\\ &\quad + P_y(T - P_T P\cos 2\varphi) + P_z(P_T G\sin 2\varphi - P_\odot E)\Big\},\end{aligned} \tag{2}$$

Here σ_0 denotes the unpolarised differential cross section, the degree of linear photon polarisation is denoted by P_T, $P_\odot$ is the right-handed circular photon polarisation and φ the azimuthal angle of the photon polarisation vector with respect to the reaction plane. An example of the first preliminary results (from approximately 100 h of running time) of the double-polarisation observable F for the $\vec{\gamma}\vec{p} \to \pi^0 p$ reaction in the energy range of 300 to 1 GeV is shown in Fig. 3 together with predictions from the SAID partial wave analysis [13] and the MAMI unitary isobar model [12].

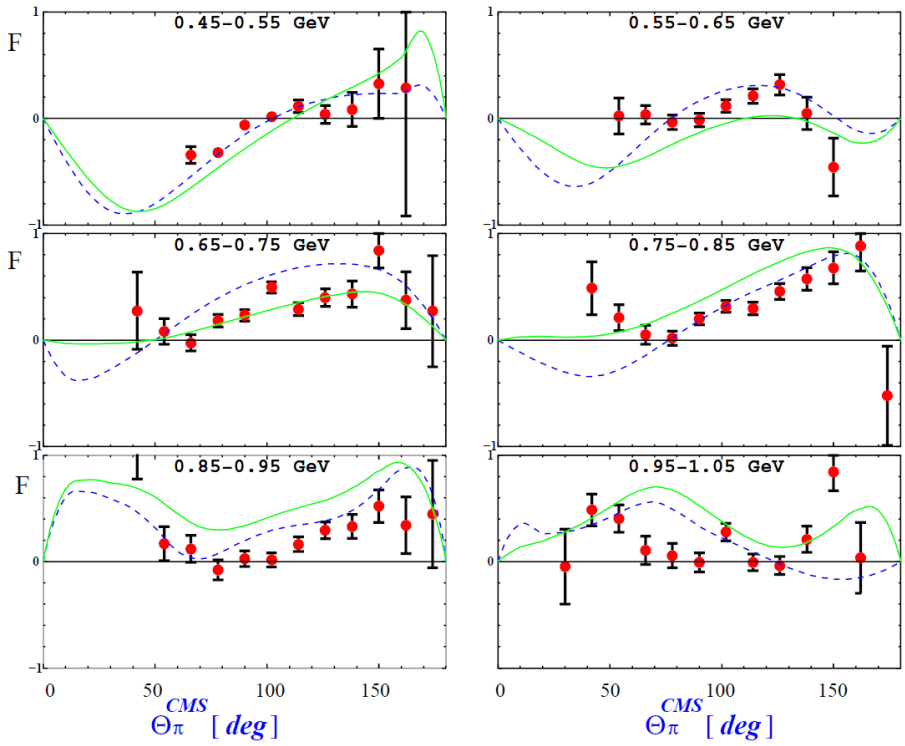

Fig. 3. First preliminary data on the double polarisation observable F in π^0 production in the photon energy range of 300 MeV to 1 GeV, compared to recent calculations (dashed: MAID, solid: SAID).

The observable F, which can only be measured with transversaly polarisedtarget in combination with circular beam polarisation, has never been measured before.

3.2.1. High-precision η photoproduction off protons and neutrons

It is well known that the $S_{11}(1535)$ has a branching ratio of 50% into the $p\eta$ decay channel, whereas the $D_{13}(1520)$ couples only very weakly to this channel. Transverse asymmetries using either a transversely polarised target in the $\gamma\vec{p} \to p\eta$ reaction or the proton recoil polarisation in the $p(e, e'\vec{p})\eta$ reaction are in particular sensitive to the interference between the S_{11} and D_{13} partial wave amplitudes. Previous data on the target asymmetry T could not be explained by overlapping Breit-Wigner functions without changing the relative phase of these two resonances by hand [17]. At MAMI, the recoil polarisation in the $p(\vec{e}, e'\vec{p})\eta$ reaction has recently been measured by the A1 collaboration ([18], see the right-hand-side of Fig. 4). These data also require a strong phase shift between the S- and D-waves, basically giving up the standard Breit-Wigner phase assignment.

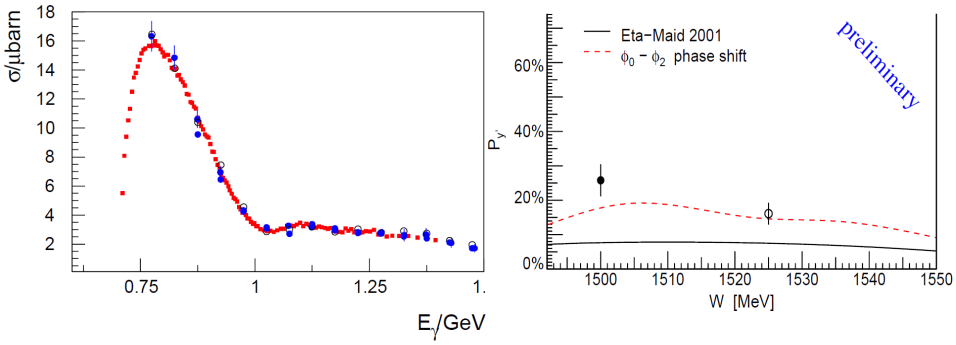

Fig. 4. Left: total cross section for the $\gamma p \to \eta p$ reaction measured with the Crystal Ball at MAMI [15] c ompared to previous results [16]. Right: Recoil polarisation for η electroproduction at $\Theta_\eta = 120^o$. Open point from [18], full point: new preliminary data [19].

With the Crystal Ball detector at MAMI, photoinduced η production can be studied with an unprecedented accuracy (see the left-hand-side of Fig. 4). The cross section data span the photon energy range from 707 to 1402 MeV and the full angular range in the c.m. frame. The accumulation of 3×10^6 events via η-decay into 3 π^0 allows a fine binning in energy (4 MeV) and angle (9 deg.). The present data agree well with previous measurements, but are markedly superior in terms of precision and energy resolution. In the energy region above $E_\gamma = 1$ GeV, a dip in the total cross section is clearly observed, especially at forward angles [15]. New data on the transverse spin observables T and F are presently under analysis.

Recently, a lot of interest has been aroused by the quasi-free photoproduction of η-mesons off neutrons bound in light nuclei. At a center of mass energy of around $W \sim 1680$ MeV a rather narrow, bump-like structure in the $D(\gamma, \eta n)p$ total cross section was observed by the GRAAL collaboration [20] and later confirmed by the LNS collaboration [21] and the CBELSA/TAPS collaboration [22]. The nature of this structure is still unknown and very different suggestions are discussed in the literature [23, 24]. With the Crystal-Ball, the quasi-free $D(\gamma, p\eta)n$ and $D(\gamma, n\eta)p$ reactions have been measured with an unprecedented accuracy. The η meson, identified via the $\eta \to \gamma\gamma$ decay, was detected in coincidence with an approximately coplanar proton or a neutron ($\Delta\Phi < 20^\circ$). Figure 5 shows preliminary excitation curves as a function of the center-of-mass energy which has been calculated in two different ways. On the left-hand-side of the picture, the total cm energy, W_{beam}, was calculated from the incident photon energy assuming a target nucleon at rest. At the right-hand-side, the cm energy, W_{true}, was determined as invariant mass of the η-nucleon final state system. The latter removes the broadening of the structure due to Fermi motion, but is limited by the experimental resolution for the neutron momentum vector. The structure is confirmed significantly and a fit of a Breit-Wigner resonance curve folded with the simulated experimental resolution yields an unfolded Breit-Wigner width of 30 ± 10 MeV. First data on polarisation observables with transverse target spin alignment, T and F, have already been measured and will help to elucidate the nature of the structure.

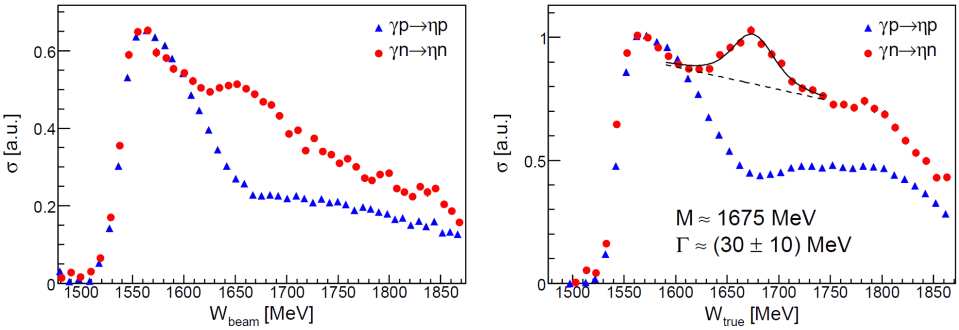

Fig. 5. Preliminary excitation curves for the quasi-free $D(\gamma, p\eta)n$ and $D(\gamma, n\eta)p$ reactions as function of the center of mass energy calculated from the beam energy assuming a target nucleon at rest (left) and from the final state invariant (right).

3.2.2. **Recoil polarimetry**

With the high intensity photon beam and the Crystal Ball detector, it is possible to measure the transverse polarisation of the recoiling proton in the $\vec{\gamma}p \to \vec{p}\pi^0$ and $\vec{\gamma}p \to \vec{p}\eta$ reactions. In this case, the differential cross section can be expressed as

$$\begin{aligned}\frac{d\sigma}{d\Omega} &= \sigma_0\Big\{1 - P_T\Sigma\cos 2\varphi + \sigma_{x'}(P_T O_{x'}\sin 2\varphi + P_\odot C_{x'}) \\ &\quad +\sigma_{y'}(P - P_T T\cos 2\varphi) + \sigma_{z'}(P_T O_{z'}\sin 2\varphi P_\odot C_{z'})\Big\}\,. \qquad (3)\end{aligned}$$

The notation for the beam polarisation, P_T and $P_\odot$, is the same as in Eq. (2). The spin components of the recoiling proton, $\sigma_{x',y',z'}$, refer to the coordinate frame with the z'-axis defined by the proton momentum vector $\vec{p}'$, the y'-axis perpendicular to the reaction plane and the x'-axis given by $\vec{x}' = \vec{y}' \times \vec{z}'$.

The polarisation transferred to the recoiling proton is measured by the analysing power of a subsequent pC scattering reaction in a carbon analyser [25, 26]. The experimental setup is shown in Fig. 6. The particle identification detector inside the Crystal-Ball is covered by a 2.5 cm thick carbon layer. Protons which undergo nuclear interactions in this layer are isolated by reconstructing the pC scattering angle. It can be determined from the reconstructed incident proton momentum vector and the hit position of the scattered proton in the Crystal Ball or TAPS calorimeter. 200 hours of data have been collected with this polarimeter using both linearly and circularly polarised photons. Preliminary results for the $C_{x'}$ observable in the $\vec{\gamma}p \to \eta\vec{p}$ reaction are shown in Fig. 6 compared with recent predictions from the MAID and SAID models. These data will provide significant new constraints on partial-wave analyses. The vertical line corresponds to a cm energy of $W_{cm} = 1680$ MeV.

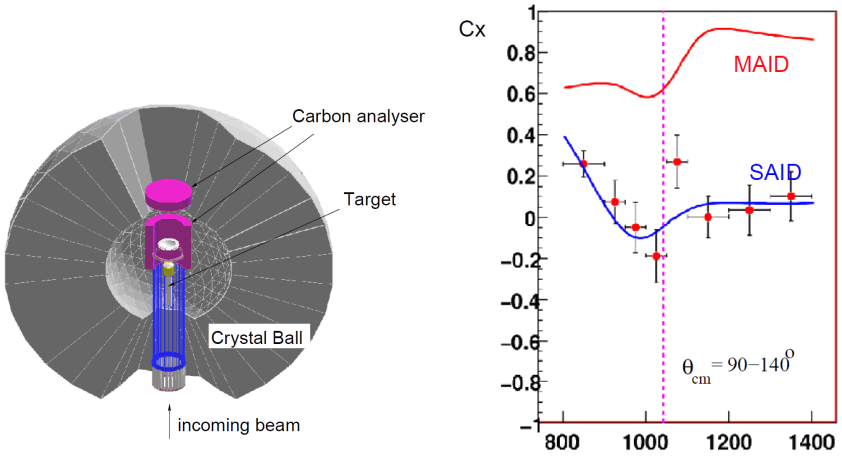

Fig. 6. Left: Setup of the recoil polarimeter. Shown are the target cell, the particle identification detector, the carbon scatterer, and the Crystal Ball. Right: Preliminary results for $C_{x'}$ in the $\vec{\gamma}p \to \eta\vec{p}$ reaction as function of the incoming photon energy. The dashed vertical line indicates a cm energy of $W = 1680$ MeV.

4. Conclusions

The Crystal Ball/TAPS detector setup at the tagged-photon facility of the MAMI C accelerator provides an ideal tool to study photoinduced reactions on nucleons and nuclei in the interesting low-energy domain of QCD. It is a hermetic photon and hadron calorimeter with full trigger capabilities for neutral particles and can be combined with polarised targets and a recoil polarimeter. Preliminary results on π^0 and η photoproduction that will have significant impact on our quantitative understanding of the structure and the dynamics of hadrons in this energy regime have been presented.

Acknowledgements

The physics program at MAMI is supported by the Deutsche Forschungsgemeinschaft (DFG) via the Sonderforschungsbereich SFB443 and the European Community-Research Infrastructure Activity under the FP6 (HadronPhysics, RII3-CT-2004-506078) and FP7 (HadronPhysicsII) programs.

References

[1] K.-H. Kaiser et al., Nucl. Instr. Meth. A **593** (2008) 159.

[2] J. C. McGeorge et al., Eur. Phys. J. A **37** (2008) 129.

[3] A. Thomas, Fizika B **20** (2011) 279 (this volume).

[4] R. Beck et al., Phys. Rev. Lett. **65** (1990) 1841.

[5] M. Fuchs et al., Phys. Lett. B **368** (1996) 20.

[6] A. Schmidt et al., Phys. Rev. Lett. **87** (2001) 232501.

[7] J. C. Bergstrom et al., Phys. Rev. C **55** (1997) 2016; Phys. Rev. C **58** (1998) 2574; Phys. Rev. C **57** (1998) 3203.

[8] V. Bernard, N. Kaiser and U. G. Meissner, Eur. Phys. J. A **11** (2001) 209.

[9] A. Gasparyan and M. F. M. Lutz, Nucl. Phys. A **848** (2010) 126; Fizika B **20** (2011) 55 (this volume).

[10] O. Hanstein, D. Drechsel and L. Tiator, Phys. Lett. B **399** (1997) 13.

[11] S. Kamalov, S. N. Yang, D. Drechsel and L. Tiator, Phys. Rev. C **64** (2001) 032201.

[12] D. Drechsel, S. S. Kamalov and L. Tiator, Eur. Phys. J. A **34** (2007) 69.

[13] R. A. Arndt, I. I. Strakovsky and R. L. Workman, Int. J. Mod. Phys. A **18** (2003) 449.

[14] A. Bock et al., Phys. Rev. Lett. **81** (1998) 534.

[15] E. F. McNicoll et al., Phys. Rev. C **82** (2010) 035208.

[16] V. Crede et al., Phys. Rev. Lett. **94** (2005) 012004.

[17] L. Tiator et al., Phys. Rev. C **60** (1999) 035210.

[18] H. Merkel et al., Phys. Rev. Lett. **99** (2007) 132301.

[19] K. Griessinger et al., to be published.

[20] V. Kuznetsov et al., Phys. Lett. B, **647** (2007) 23.

[21] F. Miyahara et al., Prog. Theor. Phys. Suppl., **168** (2007) 90.

[22] I. Jaegle et al., Phys. Rev. Lett., **100** (2008) 252002.

[23] V. A. Anisovich et al., Eur. Phys. J. A **41** (2009) 13.

[24] M. Doering and K. Nakayama, nucl-th/0909.3538v1.

[25] D. P. Watts et al., Chinese Phys. C **33** (2009) 1183.

[26] M. H. Sikora et al., Chinese Phys. C **33** (2009) 1373.

DETEKTOR CRYSTAL BALL U MAMI C: ISHODI I IZGLEDI

Sustav detektora Crystal Ball/TAPS čini zatvoren fotonski i hadronski kalorimetar za istraživanja s označenim fotonima mikrotronskog ubrzivača MAMI u Mainzu. Proučavaju se reakcije izazvane jakim snopovima polariziranih fotona energije do 1.5 GeV na nukleonima i atomskim jezgrama. U radu se opisuje oprema i izbor nedavnih ishoda mjerenja.